ORIGINAL ARTICLE

Individualized foveated rendering with eye-tracking head-mounted display

Jihwan Kim[1] · Jejoong Kim[2] · Myeongul Jung[1] · Taesoo Kwon[1] · Kwanguk Kenny Kim[1]

Abstract

Foveated rendering (FR) technology is designed to improve the efficiency of graphical rendering processes. In rendering, individualized approaches can help to balance users' experiences of visual quality and saving computational resource. However, previous studies have not rigorously examined it related with the FR techniques. To address this issue, we developed an individualized FR (IFR) method using different central vision sizes and peripheral vision resolutions across individuals in virtual reality. In three user studies with 88 participants who were divided into groups designated as "large central area (LCA)" and "small central area (SCA)," the effects of IFR were compared with those of using the full-resolution condition and the average FR condition. The results indicate that the LCA group experienced higher visual quality under the IFR and full-resolution conditions than under the average FR condition. In contrast, the SCA group exhibited comparable levels of dependent measures between the IFR and average FR conditions, but both were lower than those of the full-resolution condition. We also evaluated the computational benefits of the proposed IFR method, and the results demonstrated the effectiveness of our approach in saving resources across the two groups. Although lower-bound adjustments may be required for some users, our overall results suggest that IFR is a malleable technology for enhancing rendering efficiency in virtual reality.

Keywords Foveated rendering · Individualization · Head-mounted display · Eye-tracking · Virtual reality · User study

1 Introduction

The graphical realism of virtual reality (VR) has rapidly increased through realistic shading and lighting (McAuley et al. 2013; Overbeck et al. 2018), which has required correspondingly more computational resources for real-time rendering (Patney et al. 2016; Xiao et al. 2018). A drastic increase in computational cost can cause an end-to-end delay defined as the time required for the display to be updated (Di Luca 2010), resulting in a serious deterioration of the user's virtual experience (VE) in terms of subjective sensations such as presence, immersion, and simulator sickness (Usoh et al. 2000; Van Dam and Stephens 2018; Welch et al. 1996). Foveated rendering (FR) is a state-of-the-art technology based on the characteristics of human vision to acquire

rendering efficiency without deteriorating perceptual visual quality (Adhanom et al. 2023; Guenter et al. 2012; Korkut and Surer 2023; Vaidyanathan et al. 2014). A key concept of FR is to allocate more computational resources to the area of the display corresponding to the center of the visual field and fewer to the area of peripheral vision using parameters including designated areas and their level of quality (Levoy and Whitaker 1990). The trade-off between reducing resources and losing VE quality is considered critical in FR (Lin et al. 2002; Masnadi et al. 2022). Thus, an optimal balance should be considered to reduce the computational cost of VR rendering while maintaining a high quality of experience (Hsu et al. 2017). Several previous studies have been conducted to improve the performance of FR methods (Patney et al. 2016; Vaidyanathan et al. 2014; Xiao et al. 2018), but thus far individualized parameter settings have not yet been rigorously investigated (Hsu et al. 2017). This background shows that individualized approaches to setting principal parameters such as vision areas and visual quality in each vision area are worth exploring because they may be expected to facilitate a vivid visual experience for each user with fewer computational resources.

✉ Kwanguk Kenny Kim
  kenny@hanyang.ac.kr

1 Department of Computer Science, Hanyang University, Seoul, Republic of Korea

2 Department of Psychology, Duksung Women's University, Seoul, Republic of Korea

In this study, we propose an individualized FR (IFR) method based on individual differences in visual perception. We evaluated the effectiveness of our proposed method by comparing it with two non-personalized conditions, including using the full resolution across the entire VR display and using an average FR. In an experimental evaluation of our proposed approach, we divided a group of participants into two subgroups designated as large central area (LCA) and small central area (SCA) according to the size of the area of central vision in their visual field as measured for each individual. The proposed IFR method is designed to avoid hindering the quality of VE even when maximally conserving rendering resources. Hence, the full-resolution condition was applied as the highest quality non-personalized condition in terms of the VR equipment for comparison. In addition, because previous FR methods are not personalized based on individual parameters, the average FR was used as another non-personalized condition with a fixed level of computational resources. We evaluated the effects of this individualization by comparing our experimental results with those obtained with an averaged FR technique.

2 Related works

2.1 Human vision

Human vision comprises foveal and peripheral vision. This classification is based on the distribution of rod and cone photoreceptors in the human retina (Wald 1945). The ability to discriminate object information is mediated by the foveal area, which has a high spatial density of cone photoreceptors (Jacobson et al. 2007). The density of cones rapidly decreases toward the peripheral area of the retina. Previous studies suggested that people experience relatively high optical quality when objects fall within 30° of the fovea (Banks et al. 1991; Ogboso and Bedell 1987). However, as the eccentricity increases, the image quality deteriorates rapidly with defocusing, astigmatism, and chromatic aberrations (Banks et al. 1991; Navarro et al. 1993). Therefore, the visual quality of the peripheral vision area, which occupies most of the retina (Strasburger et al. 2011), is fundamentally lower than that of the foveal area.

Human vision differs between individuals depending on biological and personal characteristics. For example, Murray et al. (2012) demonstrated that women exhibited substantially less saturation loss in their peripheral regions than men. Other studies (Cheung and Legge 2005; Sekuler et al. 2000) investigated how peripheral visual processing declines in aging. In these studies, older adults had more difficulty tracking targets than a control group (Cheung and Legge 2005; Sekuler et al. 2000). Individual differences in color perception and eye movements including antisaccade

motions and smooth pursuit of objects have been found even within ethnically and anthropologically homogeneous groups (Emery and Webster 2019; Bargary et al. 2017).

Individualized approaches for assessing functional deficits in human vision have been provided in ophthalmology. Two basic types of individualized visual tests have been developed, including static and kinetic tests. The Humphrey and Goldman visual field tests are representative methods for detecting various visual deficits (Goldmann 1946; Trope and Britton 1987; Zahid et al. 2014). The Humphrey visual field test can be used as an automated, relatively rapid supra-threshold static test for glaucoma screening and as a static threshold test. The measurements proceed as the participant fixes their gaze at the center of their visual field, and the participant responds with a buzzer when recognizing a luminous stimulus within their field of view (FoV). This method allows quantification of visual function and subsequent follow-up for patients with glaucomatous defects in the visual field (Trope and Britton 1987). In contrast, the Goldmann visual field test reveals scotomas that static tests may fail to detect (Zahid et al. 2014). This method tests the entire visual field with a stimulus that moves continuously from the periphery to the central area (Zahid et al. 2014). An eye doctor monitors the pupil of the subject using a telescope placed behind the perimeter during the examination and then records the visible range of the target.

2.2 FoV and FR

The FoV is the portion of the visual field in which objects are simultaneously visible during steady gaze fixation (Jang et al. 2016). It is an essential factor determining the quality of VEs (Lin et al. 2002; Masnadi et al. 2022). Participants who experienced a wide FoV reported a greater sense of presence than those with a narrow FoV (Masnadi et al. 2022). Human vision consists of foveal and peripheral vision, and VR interactions can account for this characteristic by using FoV manipulation and applying differential resolutions for the foveal and peripheral areas. This FR technique improves rendering performance while maintaining visual quality (Guenter et al. 2012; Vaidyanathan et al. 2014). In various studies, the central area, the resolution of the peripheral area, and the number of layers have been used as FR parameters (Guenter et al. 2012; Vaidyanathan et al. 2014). Guenter et al. (2012) rendered three eccentricity layers around the gaze point of a user and set different resolutions depending on the layers. Vaidyanathan et al. (2014) proposed a method for achieving flexible resolution control in a rendering pipeline based on the vision layers used for FR. Subsequent studies applied additional extensions to achieve a more efficient FR while maintaining perceived visual quality. These studies classified different types of degradation of the quality of peripheral vision such as resolution

manipulation, screen-space ambient occlusion, tessellation, and ray-casting steps (Swafford et al. 2016). Along similar lines, an FR system was developed to support lower latency in a VR system with contrast preservation, multiple resolutions, and a saccade-aware temporal anti-aliasing technique (Patney et al. 2016). However, relatively few empirical studies have focused on individualized approaches (Hsu et al. 2017).

2.3 Measurement of VEs

As mentioned, there is an inherent trade-off between reducing the computational cost rendering to a VR display and the quality of the user's VE. Previous studies have evaluated VE during FR based only on a single subjective question on visual quality (Guenter et al. 2012; Hsu et al. 2017; Meng et al. 2020; Patney et al. 2016; Swafford et al. 2016). Reducing the computational resources allocated to rendering excessively tends to seriously deteriorate the quality of a VR experience in terms of realism and immersion. Thus, assessing subjective perceptions in VEs in addition to performance and behavioral tendency is important (Lin et al. 2002; Masnadi et al. 2022). These indices include simulator sickness and users' sense of presence. The latter refers to the sense of being in a virtual environment while physically located in another place (Witmer and Singer 1998) and is an essential factor in VR. Presence is related to vividness and interaction during an experience (Sheridan 1992); thus, a better VR system should provide a high degree of presence (Park et al. 2022). Simulator sickness also significantly influences the quality of users' experience with VR. Simulator sickness is a form of motion sickness occurring due to exposure to VR (Park et al. 2022), which involves various symptoms such as nausea, sweating, drowsiness, and general discomfort (Kennedy et al. 1993). Factors such as vection, graphic resolution, and FoV are related to simulator sickness (Park et al. 2022; Tian et al. 2022).

In addition to subjective feelings, various behavioral aspects in VR tasks can serve as measures of the quality of a VR experience; by measuring gaze dispersion, gaze behavior and visual attention can also be examined. Thus, a wide variety of methods have been developed based on tracking users' gaze in VR (Adhanom et al. 2020; Hirzle et al. 2019; Pai et al. 2019). Adhanom et al. (2020) identified whether users' gaze patterns changed when their FoV was reduced with a restrictor. Similarly, in the present work, we investigated differences between different FR conditions in terms of how the participants moved their gaze to perform a VR task by comparing gazing movements. Head movement can also be used as an index to assess interaction techniques and VE quality during VR experiences (Kim et al. 2017; Jang et al. 2016). Kim et al. (2017) evaluated the quality of users' experiences using data on their head rotation and

found that patterns of movement differed between different interaction conditions. The authors measured users' head rotation to determine how much the participants moved their heads to identify information about the stimulus. Response times have also been used to investigate the effects of various VR conditions (Chen et al. 2018; Jang et al. 2016). Similarly, some studies have measured accuracy to look for a trade-off with user response times (Chen et al. 2018; Jang et al. 2016).

3 Methodology for individualized foveated rendering

In this study, we developed a methodology for IFR that can guarantee VE quality with fewer computational resources. As discussed above, FR reflects structural and functional characteristics of human vision. In these techniques, the rendering areas corresponding to the visual field are divided into central and peripheral areas and a lower resolution is applied to the peripheral areas. Some relevant variables are generally considered before dividing the rendering area into segments representing users' central and peripheral vision. Given that relatively little research has been conducted on personalized FR, we considered the elements most commonly used in previous studies. For example, we applied IFR to two layers (central and peripheral) rather than to three or more. Following the Goldmann visual field test (Goldmann 1946), we also used dynamic stimuli to measure the peripheral area on the assumption of an isomorphic distribution from the center of the fovea. First, we measured the size of the central area of the participants' visual fields, and we then measured the resolution of the peripheral area. Table 1 shows pseudocode for the measurement approach we used.

To measure the size of the central area, the participants fixed their gaze on a point at the center of their FoV. If a participant did not fix their gaze on the fixation point, their entire vision was blocked, and the procedure was paused

Table 1 Pseudocode for measurement procedures

```
Interpupillary distance adjustment and eye calibration
REPEAT
        IF centralArea > minCentralArea THEN
                DECREMENT centralArea by 3.16 (per 1 second)
                IF participantResponded THEN
                        SET centralArea to maxCentralArea
                        INCREMENT numTrials by 1
                END IF
        ELSE SET centralArea to maxCentralArea
        END IF
UNTIL numTrials < 10
REPEAT
        IF peripheralResolution < maxPeripheralResolution THEN
                INCREMENT peripheralResolution by 1 (per 2 seconds)
                IF participantResponded THEN
                        SET peripheralResolution to minPeripheralResolution
                        INCREMENT numTrials by 1
                END IF
        ELSE SET peripheralResolution to minPeripheralResolution
        END IF
UNTIL numTrials < 10
```

until they were able to fix their gaze stably. As shown in Fig. 1, we distinguished two areas, including a central area with the highest quality and a peripheral area in which a 4×4 tile filter was applied as a quality deterioration. At the beginning of the measurements, we presented the measurement graphic with the highest quality for the entire area. Then, the size of the highest quality area was isomorphically decreased at a speed of 3.16° per second until the participant was able to recognize the difference in the quality of graphic between the two areas. Participants were asked to press a button on a controller as soon as they recognized the boundary. The measurement was interrupted if the participant did not respond after the size was reduced to 15°. Each trial continued for a maximum of 30 s, and the measurement was repeated ten times.

Before the measurement, we performed a practice session to ensure that the participants' responses remained stable. If the standard deviation (SD) of three practice trials was less than 10°, the practice session was terminated; otherwise, practice continued until a stable response was achieved.

We also measured the resolution of the participants' peripheral vision area (Fig. 1). First, the participants fixed their gaze on the fixation point. As in the measurement of the size of the central area, if the participants did not fix their gaze, the procedure was paused by blocking their entire visual field. Initially, the graphic was shown at the highest resolution over the entire FoV without any differences between the central and peripheral areas. Subsequently, the rendering quality in the peripheral area was reduced by applying a

downsampling filter every 2 s during the measurement. The participants were asked to press a button on a controller as soon as they recognized changes in quality. The procedure was stopped if the participant did not respond within 30 s, and the measurement session was repeated 10 times. Before the measurement, we also checked whether the participants' responses were stable in the practice trials (i.e., that the SD of the last three practice trials was < 1).

4 Pilot study

We conducted a pilot study with two objectives. The first step involved determining the parameters for the average FR conditions used in the main and extension study. As mentioned earlier, we required two non-personalized conditions that used the full resolution of the VR system over the entire visual field and an average, non-personalized FR in addition to the IFR condition. For the full resolution, the parameters were simply set according to the maximum resources of the equipment. Of note, to the best of our knowledge, no studies in the relevant literature have considered an average FR. Therefore, we conducted a pilot study to determine the size of the central area and the resolution of the peripheral area to be used as the average FR condition parameters. The second purpose of the pilot study was to determine criteria for dividing the participants into groups designated as "LCA" and "SCA." Considering the heterogeneity of human vision across different anthropological groups (Cheung and Legge
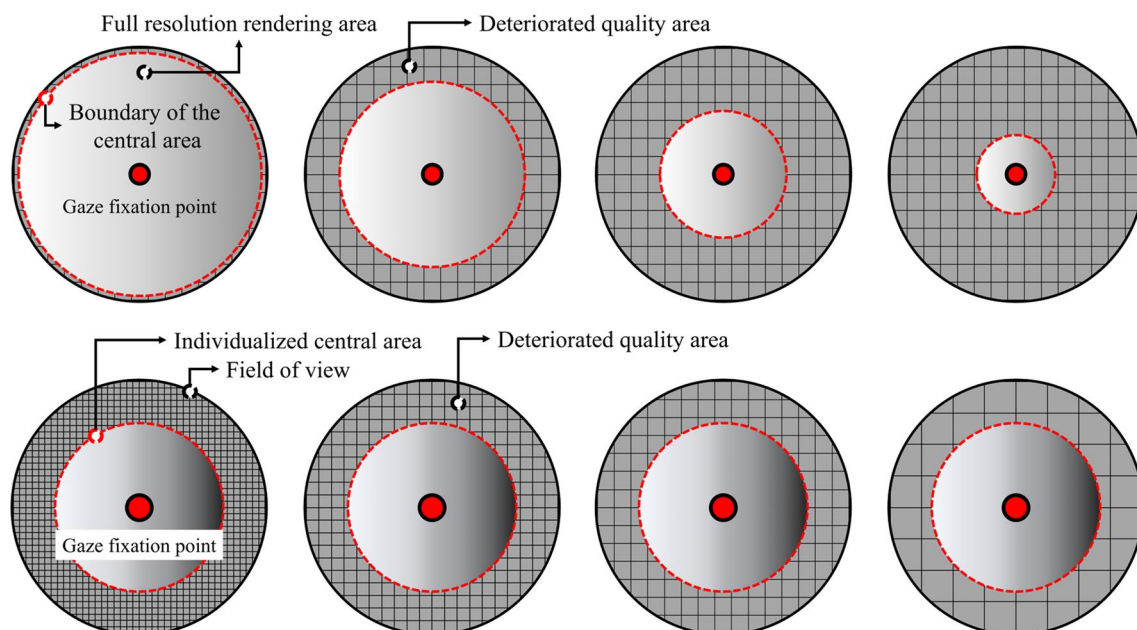

Fig. 1 Measurement process for individualized foveated rendering (top: measuring the size of the central area; bottom: measuring the resolution of the peripheral area)

2005; Murray et al. 2012; Sanda et al. 2018) or even within a given group (Bargary et al. 2017; Emery and Webster 2019), we expected that the effects of IFR would be different for each individual. However, it was not possible to reflect all individual differences in this study. Hence, we controlled all the relevant parameters except the size of the central visual area and divided our participants into two groups according to their previously recorded individual measurements of this value. Then, we looked for differences in the efficiency of IFR between the two groups.

4.1 Participants

The experiment was approved by the research site institutional review board of university. A detailed description of the procedure was provided to all participants and their written consent was obtained. Twenty participants without individual histories of problems with visual function were recruited, including 10 women and 10 men with a mean (SD) age of 24.45 (2.31). None of the participants had any mental disabilities according to the results of the symptom checklist-90-revised (SCL-90-R) (Derogatis and Unger 2010). All participants were compensated for their time at a rate of $15 per hour.

4.2 Hardware and software

We used a head-mounted display (HMD) with an eye tracker to manipulate visual quality in central and peripheral areas that varied with the participants' gaze movement. The selected HMD (HTC Vive Pro Eye, HTC, Taiwan) had a resolution of 1440×1600 pixels per eye, a refresh rate of 90 Hz, and a diagonal FoV of 110°. The eye tracker that we used (Tobii Technology AB, Sweden) had a sampling rate of 120 Hz, a trackable FoV of 110°, and an accuracy range of 0.5° to 1.1°. The HTC Vive controller was used to record the participants' responses. We used the SteamVR (Valve Co., USA) and Unity 2019.3.14f1 (Unity Technologies, USA) software frameworks to develop the VR program. The program was executed on a PC running the Windows 10 Home (64-bit) (Microsoft, USA) operating system, with a 3.70-GHz Core i5-9600KF CPU (Intel Co., USA), 32 GB of RAM (Samsung, Korea), and a GeForce GTX 1660 Ti graphics card with 6 GB of graphics memory (NVIDIA, USA).

4.3 Measurement tasks

As discussed above, the size of the participants' central areas and the resolution of their peripheral areas were measured first. These measurements were performed while the participants fixed their gaze at the center point. When the participants recognized low-quality areas within the FoV,

they responded using the VR controller. After the practice session, participants performed 10 trials to ensure a stable response. The average value of the measurement results was used to set a boundary between the central and peripheral areas. Subsequently, the resolution of peripheral area was measured. Participants responded using the VR controller as soon as they felt that the quality of their peripheral vision had changed (i.e., worsened). Again, the participants performed 10 trials after the practice session ensure a stable response. The average values of the measurement results were used to determine the quality of the peripheral area.

4.4 Procedures

The experimenter briefed the participants on information related to the experiment, including its purpose, contents, and the length of the procedure. The participants then responded to a set of demographic questionnaires including the SCL-90-R (Derogatis and Unger 2010). A practice session was conducted in a virtual classroom environment (Patney et al. 2016). After a short rest, the size of the central area and resolution of the peripheral area were measured within the experimental environment as noted above. The participants were debriefed after all processes were completed.

4.5 Results

The average size of the participants' central visual area was 76.06° (SD = 14.67). The average resolution of the peripheral area was 5.80 pixel (SD = 1.45). Individual data on the size of the central area size and peripheral resolution are provided in Table 2. The sizes of the participants' central areas did not differ significantly between males and females ($t(18) = -.870, p = .396$), nor did the average peripheral resolution ($t(18) = 1.248, p = .228$). We determined the average size of the central visual area to be 76.06° (the overall average), which was used to divide the participants in the main study into two groups and for the average FR condition in the main study. The filter size for quality deterioration was set as five pixels, which was used for the average FR condition. We rounded the average resolution down to obtain an integer value for use in the main study.

5 Main study

In the main study, we evaluated the effect of the proposed IFR in comparison with the full-resolution and average FR conditions in both the LCA and SCA groups. The experimental design was a 3 (conditions: IFR, average FR, and full resolution) $\times$ 2 (groups: LCA and SCA participants) within-subjects design. For the average FR condition, we used the central area size and peripheral resolution from

Table 2 Measurement results for mean (standard deviation) of the central area and the resolution of the peripheral area in the pilot study

Participant number	Size of central area (°)	Resolution of peripheral area (pixel)	Gender
1	75.50	3.50	Female
2	90.25	5.00	Female
3	68.00	6.50	Female
4	50.75	6.50	Male
5	81.35	7.50	Female
6	77.45	5.50	Female
7	71.20	6.00	Female
8	68.05	9.50	Male
9	84.60	5.50	Male
10	48.20	8.00	Male
11	90.05	5.00	Male
12	80.45	4.50	Female
13	85.40	4.00	Female
14	41.25	6.50	Male
15	93.60	5.00	Male
16	76.80	6.50	Male
17	82.00	6.50	Female
18	77.70	5.00	Female
19	87.40	4.00	Male
20	91.15	5.50	Male
Average (male)	73.19 (19.84)	6.20 (1.60)	
Average (female)	78.93 (6.52)	5.40 (1.24)	
Average (all)	76.06 (14.67)	5.80 (1.45)	

the pilot study. In the full-resolution condition, we used the maximum resources of the HMD hardware. In the IFR condition, participants with central sizes larger and smaller than 76.06° were assigned to the LCA and SCA groups, respectively. The dependent variables that we measured included the participants' sense of presence, simulator sickness, perceptual sensations, task performance, gaze dispersion, and head movements.
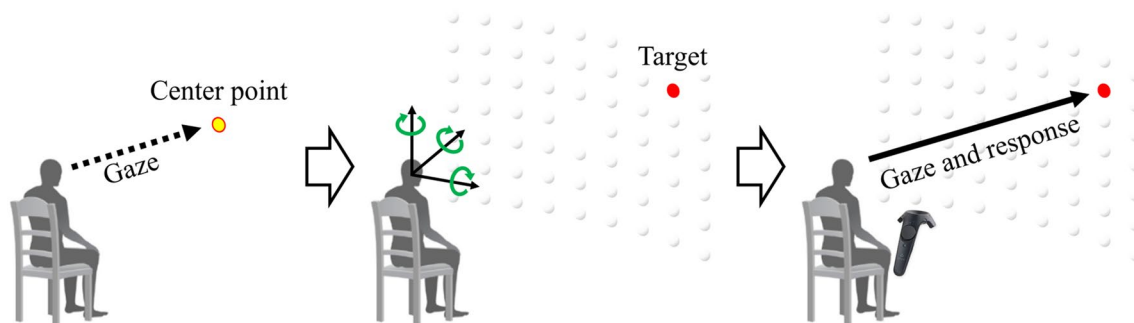
5.1 Participants

All participants were given a detailed description of the procedure and completed written consent forms. A total of 30 participants (8 women and 22 men) without any history of visual deficiency were recruited for the main study. The mean age of participants was 24.37 years (SD = 2.16). None of the volunteers had any mental disabilities as determined by the results of administering the SCL-90-R (Derogatis and Unger 2010). All participants were compensated at a rate of $15 per hour for their time. Fifteen of the 30 participants (4 women and 11 men) with an average age of 24.40 were allocated to the LCA group, and the remaining 15 participants (4 women and 11 men) with an average age of 24.33 were allocated to the SCA group.

5.2 Measurement tasks

As described above, we first measured the size of the central visual area and resolution of the peripheral area of each participant.

5.3 Evaluation tasks

To evaluate the participants' VEs in the three conditions for each group, we used a visual task (Fig. 2) that consisted of two types depending on the target stimulus. One was a color-recognition task (Jang et al. 2016) in which the participants identified the color (red or blue) of a randomly appearing target. The second task focused on shape recognition (Chen et al. 2018) to identify the shape (sphere or tetrahedron) of a randomly appearing target. The specific settings for the visual tasks were similar to those used by Jang et al. (2016). All 62 stimuli were arranged over a 9 × 7 (horizontal × vertical) spherical coordinate system (horizontal range of −40° to +40°; vertical range of −30° to +30°), excluding the center point, and had the same 10° radial distance. In each trial, a point was displayed at the center of the virtual environment along with a sound effect to align the participant's

Fig. 2 Concept of the visual task used in the main study

gaze. If the participant gazed at the target point, it then disappeared. A stimulus randomly appeared in one of the 62 locations. The participants pressed the left or right button on the controller as soon as they could discriminate the color or shape of the stimuli. The trials varied from 0.5 to 1.5 s in duration.

5.4 Dependent measurements

5.4.1 Presence questionnaire

The participants' sense of presence during the VE was assessed using the presence questionnaire (PQ) (Witmer and Singer 1998), which consisted of 18 items for involvement/control, resolution, interface quality, and naturality scored on a 7-point Likert scale (1 = not at all, 7 = completely).

5.4.2 Simulator sickness questionnaire

Simulator sickness was assessed using the simulator sickness questionnaire (SSQ) (Kennedy et al. 1993). The questionnaire comprises a 16-item symptom checklist scored on a 4-point Likert scale (0 = not at all, 3 = severe).

5.4.3 Perception questionnaire

To ensure that the participant recognized the boundary between the central and peripheral areas, we used a questionnaire on area perception (APQ) with a 7-point Likert scale (1 = not at all, 7 = completely). The questionnaire asked, "Did you notice that the high-quality area of vision was narrow in the virtual environment?" In addition, a questionnaire on the participants' perceptions of deterioration of visual quality (DPQ) with a 7-point Likert scale (1 = not at all, 7 = completely) was used to evaluate whether the participants perceived the reduced visual quality of the peripheral areas. The question used was "Did you notice that the quality of certain areas of the HMD was poor during the virtual experience?".

5.4.4 Task performance

Response time was the main dependent measure of performance on the tasks. For each stimulus, the participants' response time was recorded as the time elapsed between the moment that they gazed at the center and the moment when they pressed a button on the controller, and the response times for 62 stimuli were averaged.

The accuracy (% of correct answers) was also recorded. Our results did now show any trade-off between response time and accuracy, and accuracy was quite high overall (> 98.73%, SD = 1.04), presumably because the task itself

was simple. Thus, we did not consider accuracy as a key dependent variable.

5.4.5 Gaze dispersion

Gaze dispersion represents the length of the trajectories along which a user moves their gaze to identify a target during a VE. The distance between the x- and y-coordinates of the point at the center of their gaze in the current and previous frames was calculated for each frame, and the gaze dispersion was calculated as the sum of these distances. In each trial, the gaze tracking process started with a gaze alignment and ended with the participant's response.

5.4.6 Head movements

When the participants rotated their heads to identify the stimulus, their head rotation was measured as the sum of the rotation angles, i.e., the yaw, pitch, and roll directions (Kim et al. 2017). The process of measuring head rotation began with the gaze alignment at the beginning of each trial and ended with the response of the participant.

5.5 Procedures

The experimenter briefed the participants on the purpose of the experiment as well as its duration, procedures, and the equipment to be used (Fig. 3). The participants then responded to a demographic questionnaire and the SCL-90-R (Derogatis and Unger 2010). Subsequently, a practice session was conducted in the experimental environment (a virtual classroom). After resting for 3 min, the participants performed a measurement task with their individualized IFR parameters. Then, the evaluation tasks (color-recognition and shape-recognition tasks) were conducted with IFR, average FR, and full-resolution conditions in the same experimental environment (a virtual classroom). All the processes were counterbalanced. After completing each condition, the participants responded to questionnaires on sense of presence, simulator sickness, and perception. Lastly, the participants were debriefed. The entire procedure lasted approximately 2 h.

5.6 Data analysis

All data were analyzed using the IBM SPSS 25.0 (SPSS Inc., USA) software package. The average values of the color- and shape-recognition tasks were used for the analysis. Normality was evaluated based on the skewness and kurtosis using a Kolmogorov–Smirnov test. Sphericity was evaluated using Mauchly's test. Repeated measures of analysis of variance (RM ANOVA) for the three FR conditions (IFR, average FR, and full resolution) × two groups (LCA and SCA) were
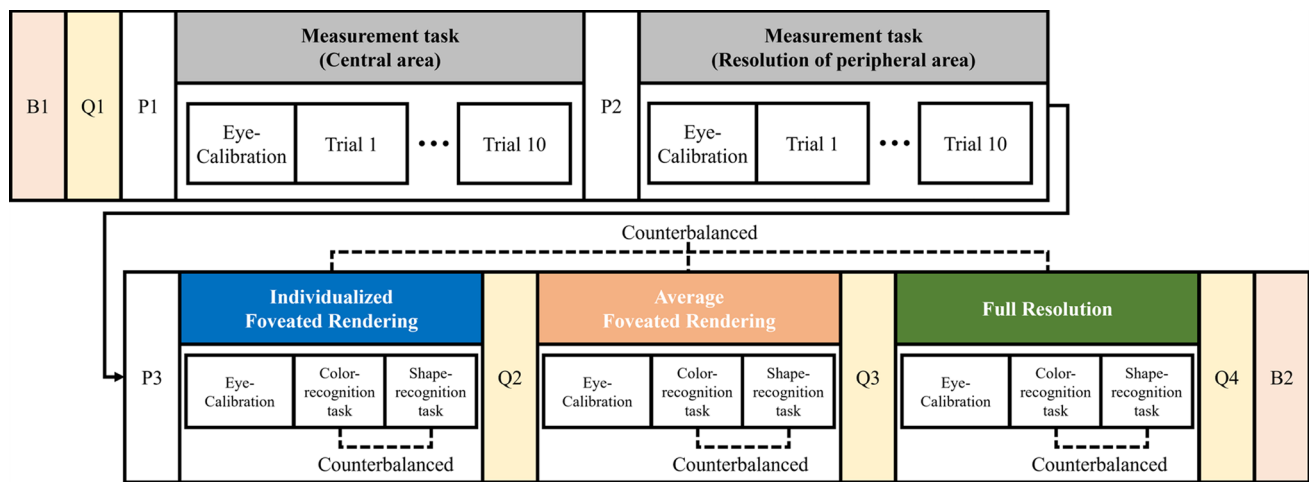
Fig. 3 Experimental procedure for the main study. (B1, briefing; B2, debriefing; P1, practice session for the measurement of the central area; P2, practice session for the resolution of the peripheral area; P3, practice session for the evaluation task; Q1, pre-questionnaire; Q2, Q3, Q4, post-questionnaires)

conducted to examine differences depending on the FR condition and group. If an interaction effect was found, post hoc analyses were conducted for each group using a paired *t*test for multiple comparisons. The level of statistical significance was set at $p < 0.05$.

5.7 Results

5.7.1 Individual measurement results

In the main study, the average central area of all participants was 79.44° (SD = 10.10), and the average resolution of the peripheral area was 4.97 (SD = 0.96). The individual measurement results are presented in Table 3. The average central area of the LCA group was 88.30° (SD = 4.61), and the average resolution of the peripheral area was 4.93 (SD = 1.16). In the SCA group, the average central area was 70.57° (SD = 4.65), and the average resolution of the peripheral area was 5.00 (SD = 0.76). The central area of the LCA group was significantly wider than that of the SCA group $(t(28) = -10.487, p < .001)$.

5.7.2 Presence questionnaire

A significant main effect of the FR conditions $(F(2, 56) = 9.982, p < .001, \eta^2 = .263)$ was observed on the presence score. However, the groups showed no significant main effect $(F(1, 28) = 1.973, p = .171, \eta^2 = .066)$. Interaction between the FR conditions and groups was significant $(F(2, 56) = 4.181, p < .05, \eta^2 = .130)$. A post hoc analysis (*t* test) for multiple comparisons was also conducted. As shown in Fig. 4A, in the LCA group, the presence scores of the IFR and full-resolution conditions were higher than

those of the average FR condition $(t(14) = -2.564, p < .05; t(14) = -2.601, p < .05)$, whereas no significant differences were found between the IFR and full-resolution conditions $(t(14) = -.712, p = .488)$. In the SCA group, the presence score under the full-resolution condition was significantly higher than under both the IFR $(t(14) = -3.910, p < .01)$ and average FR $(t(14) = -2.898, p < .05)$ conditions. The difference between the average FR and IFR was not significant $(t(14) = 1.247, p = .233)$.

5.7.3 Simulator sickness questionnaire

There were no significant main effects of the FR condition $(F(2, 56) = .115, p = .891, \eta^2 = .004)$ or of the groups $(F(1, 28) = 1.495, p = .232, \eta^2 = .051)$ on the simulator sickness scores. The results for simulator sickness are shown in Fig. 4B. Interaction between the FR condition and group was not significant $(F(2, 56) = .758, p = .473, \eta^2 = .026)$.

5.7.4 Perception questionnaire

Significant main effects of the FR condition $(F(2, 56) = 7.298, p < .01, \eta^2 = .207)$ and group $(F(1, 28) = 8.857, p < .01, \eta^2 = .240)$ on the APQ were found. Importantly, interaction between the FR condition and groups was also significant $(F(2, 56) = 5.074, p < .01, \eta^2 = .153)$. A post hoc analysis of multiple comparisons is presented in Fig. 4C. In the LCA group, the scores obtained under the IFR and full-resolution conditions were significantly lower than those under the average FR condition $(t(14) = 3.035, p < .01; t(14) = 2.280, p < .05)$. That is, the participants did not notice a significant difference in the vivid area

Table 3 Mean measurement results (standard deviation) of the central area and the resolution of the peripheral area in the main study

Participant number	Size of central area (°)	Resolution of peripheral area (pixel)	Group
1	83.09	6.00	LCA
2	61.38	6.00	SCA
3	78.37	6.00	SCA
4	62.84	5.00	SCA
5	69.78	5.00	SCA
6	73.04	6.00	SCA
7	72.94	4.00	SCA
8	71.35	6.00	SCA
9	64.54	5.00	SCA
10	71.71	5.00	SCA
11	71.39	4.00	SCA
12	74.17	5.00	SCA
13	93.33	4.00	LCA
14	68.54	5.00	SCA
15	70.02	5.00	SCA
16	94.54	4.00	LCA
17	73.01	4.00	SCA
18	90.63	5.00	LCA
19	84.37	6.00	LCA
20	75.41	4.00	SCA
21	91.70	5.00	LCA
22	81.07	4.00	LCA
23	90.40	3.00	LCA
24	84.13	6.00	LCA
25	93.52	4.00	LCA
26	86.81	4.00	LCA
27	88.65	6.00	LCA
28	86.62	4.00	LCA
29	82.06	7.00	LCA
30	93.63	6.00	LCA
Average (LCA)	88.30 (4.61)	4.93 (1.16)	
Average (SCA)	70.57 (4.65)	5.00 (0.76)	
Average (entire)	79.44 (10.10)	4.97 (0.96)	

LCA Large central area; *SCA* Small central area

between the IFR and full-resolution conditions ($t(14) = -.225, p = .825$). This result also indicates that the perceived vivid area in the average FR condition was narrower than that in the IFR and full-resolution conditions. In the SCA group, the scores from the full-resolution condition were significantly lower than those from the average FR ($t(14) = 2.824, p < .05$) and IFR ($t(14) = 3.332, p < .01$) conditions. There was no significant difference between the average FR and IFR conditions ($t(14) = -1.362, p = .195$), indicating that the perceived vivid area in the average FR and IFR conditions was narrower than those in the full-resolution condition.

A significant main effect of the FR conditions on the DPQ score was found ($F(2, 56) = 5.767, p < .01, \eta^2 = .171$). However, no significant main effect of the groups ($F(1, 28) = 2.278, p = .142, \eta^2 = .075$) was observed. In addition, there was no interaction between the FR conditions and groups ($F(2, 56) = 1.772, p = .179, \eta^2 = .060$). The results of the DPQ are shown in Fig. 4D.

5.7.5 Response time

The main effect of the FR condition on the response time (Table 4) was not significant ($F(2, 56) = 1.459, p = .241, \eta^2 = .050$), whereas a significant main effect of the groups was observed ($F(1, 28) = 4.662, p < .05, \eta^2 = .143$, Table 4). There was no significant interaction between the FR conditions and groups ($F(2, 56) = .476, p = .624, \eta^2 = .017$).

5.7.6 Gaze dispersion

There were no significant main effects of the FR conditions ($F(2, 56) = .574, p = .566, \eta^2 = .020$) and groups ($F(1, 28) = 3.564, p = .069, \eta^2 = .113$) on the gaze dispersion (Table 4). Interactions between the FR conditions and groups were also not significant ($F(2, 56) = 1.310, p = .278, \eta^2 = .045$). The gaze dispersion results suggest that there was no significant difference in total gaze movement across the FR conditions.

5.7.7 Head rotation

There were no significant main effects of the FR condition ($F(2, 56) = .147, p = .864, \eta^2 = .005$) and group ($F(1, 28) = 3.278, p = .081, \eta^2 = .105$) on the head rotation (Table 4). There were no interactions between the FR conditions and groups ($F(2, 56) = .160, p = .852, \eta^2 = .006$). Similar to gaze dispersion, the results for head rotation suggest that there was no significant difference in total head rotation across FR conditions.

6 Extension study

In the main study, we found that the LCA group experienced a similar level of VE quality under the IFR and full-resolution conditions. Because this result was observed in a restricted experimental environment, we conducted an additional study to confirm these findings with a more general game application. To this end, we evaluated the proposed IFR methodology again using a first-person shooter (FPS) game similar to an existing game called VirtuaCop2 (SEGA Games, Japan). We also calculated the exact number of pixels that could be saved using the proposed method.
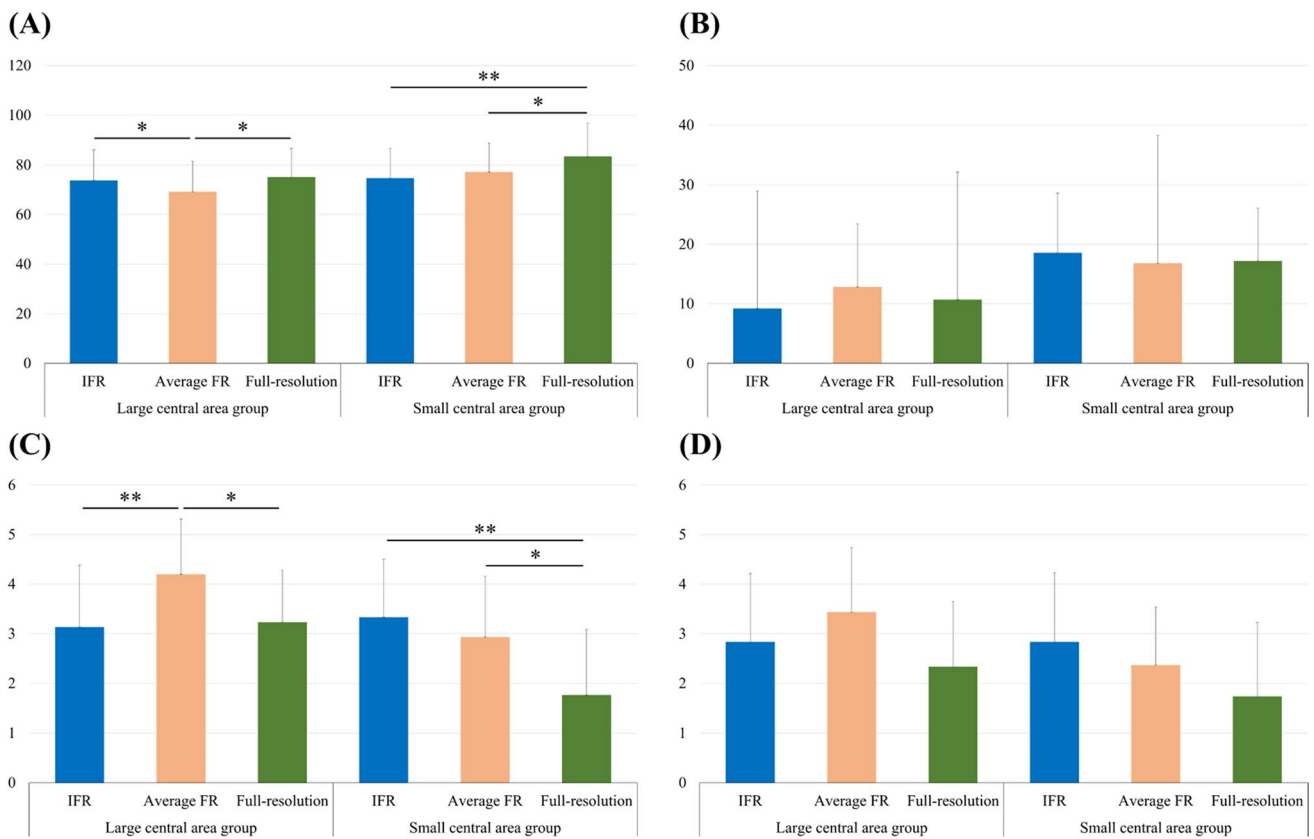
(A)

(B)

(C)

(D)

Fig. 4 **A** Results for the presence, **B** simulator sickness, **C** area perception, and **D** perception of deterioration of visual quality. *Significant at $p < .05$, **significant at $p < .01$. Note: IFR, Individualized foveated rendering; Average FR, Average foveated rendering

Table 4 Mean behavioral results (standard deviation) including the response time, gaze dispersion, and head rotation

	LCA group			SCA group		
	Individualized foveated rendering	Average foveated rendering	Full resolution	Individualized foveated rendering	Average foveated rendering	Full resolution
Response time (s)	0.82 (0.11)	0.84 (0.11)	0.82 (0.08)	0.94 (0.17)	0.94 (0.17)	0.92 (0.18)
Gaze dispersion (cm)	18.12 (3.85)	18.44 (3.51)	18.19 (3.63)	20.59 (3.59)	19.64 (3.39)	21.04 (3.46)
Head rotation (°)	1401.17 (629.17)	1463.32 (669.50)	1428.88 (601.30)	1924.15 (820.68)	1925.14 (953.29)	1972.73 (1056.51)

LCA Large central area; *SCA* Small central area

6.1 Participants

All participants were provided a detailed description of the experimental procedures and completed written consent forms. Thirty-eight participants (15 women and 23 men) with no history of visual deficiency were recruited. Their mean age was 27.00 years (SD = 5.48). None of the volunteers had any mental disabilities and they were compensated $15 per hour for their participation. Twenty of the 38 participants (5 women and 15 men) were assigned to the LCA group (mean age = 26.65), and the others (10 women and 8 men) were assigned to the SCA group (mean age = 27.39).

6.2 VR-based first-person shooter game

We developed a VR game similar to Virtual Cop2 (SEGA Games, Japan) for the extension study (Fig. 5). In the game,
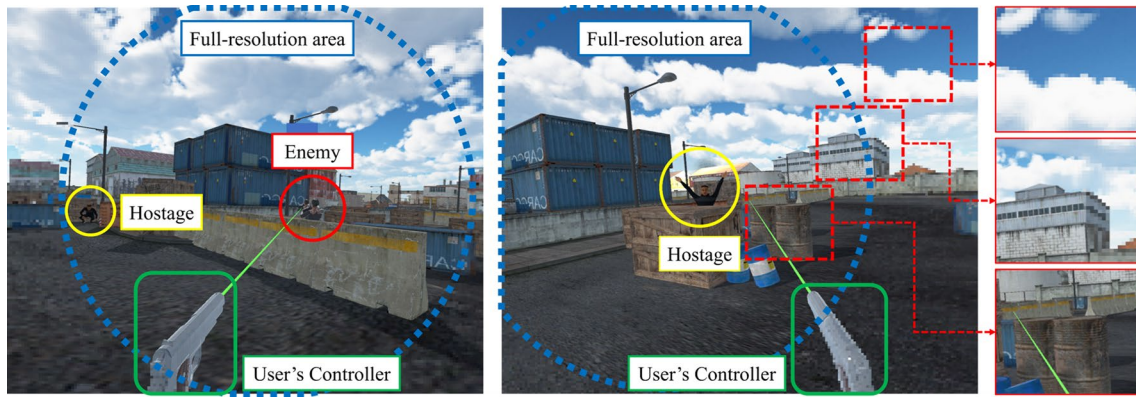
Fig. 5 VR-based first-person shooter game with individualized foveated rendering condition

the player was tasked with reaching a specific designated location to distinguish an enemy target from simulated hostages and then firing at the former. A target board with the word "Start" was displayed in front of the players in the virtual space just before they began the game. If the participant hit the target correctly, the game began. When the participants arrived at the shooting position, five hostages and five enemies appeared in the 3D game area. If the participants successfully suppressed all the enemies at that location by firing at them, the players then moved on to the next position. The targets at each position were arranged over a 10×1 (horizontal $\times$ vertical) spherical coordinate system (horizontal range of $-55°$ to $+55°$), and all targets had the same $10°$ radial distance. Because there were 10 shooting positions, a total of 50 enemies and 50 hostages appeared with corresponding sound effects.

6.3 Calculation of reduced number of pixel

The rendering cost was calculated for the IFR condition with the values of each individual based on their personal measurement results. Assuming that the distance between the center gaze point and the eyes is V, the angle between the center gaze point and the peripheral point is e, and the maximum angle depending on the FoV of the HMD is e_{max}, then the central region A_c, the peripheral region A_p, and the total region A_t are calculated as follows.

$$A_t = \pi\{\tan(e_{max}) \times V\}^2; A_c = \pi\{\tan(e) \times V\}^2; A_p = A_t - A_c.$$

Assuming that the measurement results for the resolution of the peripheral area are r and the maximum number of pixels depending on the HMD is P_{max}, then the number of pixels in the peripheral area P_p, the number of pixels in the central area P_c, and the number of pixels used for rendering P_{used} are related as given below.

$$P_p = P_{max} \times \frac{A_p}{A_t} \times \frac{1}{r^2}; P_c = P_{max} \times \frac{A_c}{A_t}; P_{used} = \frac{P_p + P_c}{P_{max}}.$$

The number of reduced pixels used for rendering was calculated according to these formulas.

6.4 Dependent measurements and conditions

We used the same dependent measurements as in the main study, including sense of presence, simulator sickness, perception, task performance, gaze dispersion, and head movement. We also used the same conditions and parameters applied in the main study, including the IFR, average FR, and full-resolution conditions.

6.5 Procedures

After the experimenter briefed the participants about the experiment, a VR practice session was conducted. Then, the IFR parameters were measured. Subsequently, the participants played the VR-based FPS game under the IFR, average FR, and full-resolution conditions in a counterbalanced order. After each condition, the participants responded to the questionnaires (presence, simulator sickness, and perception). They were then debriefed at the end of the experiment. The procedure lasted approximately 2 h.

6.6 Data analysis

RM ANOVA were conducted for the three FR conditions (IFR, average FR, and full resolution) $\times$ two groups (LCA and SCA) to examine the differences depending on the FR condition and group. If an interaction effect was found, post hoc analyses were conducted for each group using a paired t test for multiple comparisons. The level of statistical significance was set at $p < 0.05$.

6.7 Results

6.7.1 IFR measurement and results of reduced rendering pixels

The average central area of the LCA group was 85.11° (SD = 5.03), and the average resolution of the peripheral area was 5.10 (SD = 1.21). Given that 100% of the pixels were required for the full-resolution condition, the results suggest that the proposed IFR condition required 44.40% (SD = 7.46) as many pixels to be rendered. Table 5 shows the individual results for the LCA group.

The average central area of the SCA group was 64.00° (SD = 8.48), and the average resolution of the peripheral area was 5.54 (SD = 1.05). Given that 100% of the pixels are required for the full-resolution condition, the results suggest that the current IFR condition required 23.51% (SD = 5.94) as many pixels to be rendered (Table 6). It also suggests that the current IFR condition required 71.60% (SD = 18.09) pixels, given that 100% of the pixels are required for the average FR condition.

6.7.2 Presence questionnaire

The results of a 3×2 ANOVA showed significant main effects of the FR condition ($F(2, 72) = 5.941, p < .01, \eta^2 = .142$) on the presence score. However, no significant main effect of the groups was found ($F(1, 36) = .092, p = .763, \eta^2 = .003$). Interaction between the FR conditions and groups was significant ($F(2, 72) = 6.018, p < .01, \eta^2 = .143$). The results of t test conducted as the post hoc analysis for multiple comparisons are presented in Fig. 6A. The LCA participants reported experiencing a significantly lower presence under the average FR condition than under the IFR ($t(19) = -3.801, p < .001$) and full-resolution conditions ($t(19) = -4.833, p < .001$). There was no significant difference between IFR and full-resolution condition ($t(19) = -.388, p = .702$). In the SCA group, there were no significant differences between the IFR and average FR conditions ($t(17) = -.987, p = .338$), IFR and full-resolution conditions ($t(17) = -1.468, p = .160$), or between the average FR and full-resolution conditions ($t(17) = -.610, p = .550$).

6.7.3 Simulator sickness questionnaire

The main effect of the FR condition was not significant ($F(2, 72) = .203, p = .817, \eta^2 = .006$) and the groups ($F(1, 36) = .330, p = .569, \eta^2 = .009$). Interactions between the FR conditions and groups was not significant, either ($F(2, 72) = 1.358, p = .264, \eta^2 = .036$). The results for simulator sickness are shown in Fig. 6B.

Table 5 Measurement results of the large central area group in the extension study

Participant number	Central area (°)	Resolution of peripheral area (pixel)	Used pixel compared with full-resolution condition (%)
1	88.10	5.00	48.05
2	91.92	4.00	55.40
3	90.93	4.00	53.73
4	78.79	6.00	34.93
5	85.13	5.00	43.70
6	80.08	5.00	37.23
7	79.85	8.00	35.36
8	76.44	5.00	33.19
9	89.96	4.00	52.15
10	83.43	4.00	42.78
11	85.71	4.00	45.82
12	92.18	4.00	55.85
13	79.25	4.00	37.76
14	80.15	7.00	36.04
15	79.27	7.00	34.99
16	88.78	4.00	50.30
17	89.40	5.00	50.09
18	88.64	6.00	48.24
19	87.62	6.00	46.64
20	86.62	5.00	45.83
Average (standard deviation)	85.11 (5.03)	5.10 (1.21)	44.40 (7.46)

Table 6 Measurement results of the small central area group in the extension study

Participant number	Central area (°)	Resolution of peripheral area (pixel)	Used pixel compared with full-resolution condition (%)
1	71.58	6.00	27.55
2	58.06	6.00	17.46
3	69.45	7.00	25.11
4	74.77	4.00	33.09
5	73.52	5.00	30.27
6	68.51	6.00	24.88
7	56.07	4.00	19.28
8	62.83	4.00	23.40
9	62.88	5.00	21.59
10	59.19	6.00	18.15
11	70.19	3.00	32.63
12	72.19	6.00	28.12
13	52.13	4.00	17.25
14	68.95	6.00	25.25
15	57.10	5.00	17.93
16	55.72	4.00	19.09
17	46.13	5.00	12.53
18	72.76	5.00	29.55
Average (standard deviation)	64.00 (8.48)	5.54 (1.05)	23.51 (5.94)
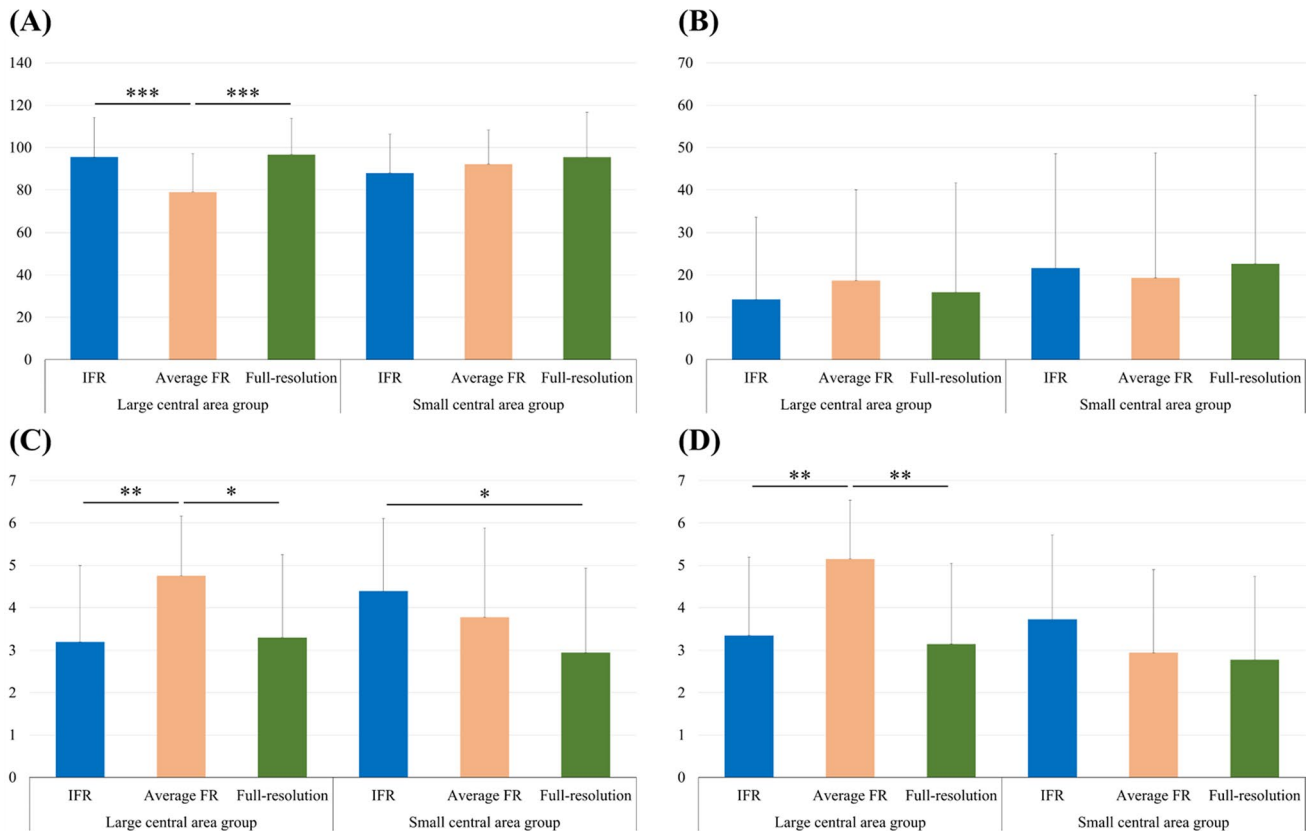
Fig. 6 Results for **A** sense of presence, **B** simulator sickness, **C** area perception, and **D** perceived deterioration of visual quality. *Significant at $p < .05$, **significant at $p < .01$, ***significant at $p < .001$.

Note: IFR, Individualized foveated rendering; Average FR, Average foveated rendering

6.7.4 Perception questionnaire

A significant main effect of the FR condition ($F(2, 72) = 4.561, p < .05, \eta^2 = .112$) on the APQ score was observed. Differences of the group main effect were not significant ($F(1, 36) = .013, p = .909, \eta^2 = .000$). However, interaction between the FR condition and groups was significant ($F(2, 72) = 4.292, p < .05, \eta^2 = .107$). The results of the post hoc t test for multiple comparisons are shown in Fig. 6C. The results indicated that the LCA participants felt a narrower vivid area under the average FR condition than under the IFR ($t(19) = 2.843, p < .01$) and full-resolution conditions ($t(19) = 2.332 p < .05$). The difference between the IFR and full-resolution conditions ($t(19) = -.282, p = .781$) was not significant. In the SCA group, there were no significant differences between the IFR and average FR ($t(17) = 1.257, p = .226$) or between the average FR and full resolution ($t(17) = 1.399, p = .180$). However, these participants felt significantly narrower vivid areas under the IFR conditions than under the full-resolution conditions ($t(17) = 2.496, p < .05$).

In terms of the DPQ score, the results show significant main effects of the FR condition ($F(2, 72) = 4.761, p < .05, \eta^2 = .117$). The main effect of the groups was not significant ($F(1, 36) = 2.779, p = .104, \eta^2 = .072$). Interaction between the FR condition and group was significant ($F(2, 72) = 7.133, p < .01, \eta^2 = .165$). Figure 6D shows the results of the post hoc t test. In the LCA group, participants felt that the peripheral area quality under the average FR condition was significantly worse than that under the IFR ($t(19) = 3.327, p < .01$) and full-resolution conditions ($t(19) = 3.651, p < .01$). There was no significant difference between the IFR and full-resolution conditions ($t(19) = .490, p = .629$). In the SCA group, there were no significant differences between the IFR and average FR ($t(17) = 1.740, p = .100$), IFR and full resolution ($t(17) = 1.836, p = .084$), or average FR and full-resolution conditions ($t(17) = .338, p = .740$).

6.7.5 Response time

There were no significant main effects of the FR condition ($F(2, 72) = .610, p = .546, \eta^2 = .017$) nor of the groups ($F(1, 36) = .248, p = .621, \eta^2 = .007$) on the response time. Moreover, there was no interaction between the FR condition and groups ($F(2, 72) = 1.895, p = .158, \eta^2 = .050$). Table 7 shows the results and indicates that the participants did not present a longer response time under the IFR condition during the task than under the other conditions.

6.7.6 Gaze dispersion

There were no significant main effects of the FR conditions ($F(2, 72) = .795, p = .456, \eta^2 = .022$) nor of the groups ($F(1, 36) = 2.148, p = .151, \eta^2 = .056$) on gaze dispersion. Interaction between the FR condition and groups was not significant ($F(2, 72) = 1.283, p = .283, \eta^2 = .034$). Table 7 shows the results; there was no significant difference in the total gaze movement across the FR conditions.

6.7.7 Head rotation

There were no significant main effects of the FR condition ($F(2, 72) = 1.583, p = .212, \eta^2 = .042$) nor of the groups ($F(1, 36) = .085, p = .773, \eta^2 = .002$) on the head rotation. Interaction between the FR condition and group was not significant ($F(2, 72) = .310, p = .734, \eta^2 = .009$). Table 7 shows the results; there was no significant difference in total head rotation across the FR conditions.

7 Discussion

In this study, we proposed an individual approach to FR and evaluated its usefulness in comparison with conventional average FR and full-resolution conditions. Overall, the results showed that the VE under the IFR condition was comparable to that under the full-resolution condition in the

Table 7 Behavioral results of the extension study in terms of mean values (standard deviation) including the response time, gaze dispersion, and head rotation

	LCA group			SCA group		
	Individualized foveated rendering	Average foveated rendering	Full resolution	Individualized foveated rendering	Average foveated rendering	Full resolution
Response time (s)	1.81 (0.38)	1.76 (0.39)	2.05 (1.20)	1.64 (0.43)	2.02 (0.77)	1.73 (0.38)
Gaze dispersion (cm)	22.37 (10.82)	25.84 (13.96)	22.80 (8.83)	19.14 (4.69)	19.47 (3.99)	21.31 (11.23)
Head rotation (°)	2990.24 (1011.14)	3203.54 (835.73)	2890.64 (904.79)	2938.93 (748.42)	3024.54 (835.73)	2904.54 (817.69)

LCA Large central area; *SCA* Small central area

LCA group in both the main experiment and the extension study. Furthermore, it was significantly better than that under the average FR condition. These results suggest that IFR can guarantee a level of VE comparable to that of full resolution with approximately half the computational resources or less. However, in the SCA group, the effects of the IFR were not evident. In this group, although the IFR condition was not as effective as full resolution, it was comparable to or better than the average FR. Overall, the results show that our proposed IFR was efficient in terms of VE quality with reduced computational resources.

The rendering resources allocated to the peripheral area were reduced using our proposed IFR method. However, the quality of the users' VE did not deteriorate in the LCA group. One possible reason for such a good ratio of quality to computational resources may be that we used an HMD device that supports eye-tracking technologies (Stengel et al. 2015). That is, when a participant moves their gaze, the central area moves accordingly, which makes it difficult to recognize degradation of the visual quality of the periphery (Guenter et al. 2012; Patney et al. 2016). This does not suffice, however, because human vision is quite heterogeneous across individuals or ethnic groups (Bargary et al. 2017; Cheung and Legge 2005; Emery and Webster 2019; Sekuler et al. 2000). Thus, each user might perceive a different quality of VE even under the same FR parameters. Therefore, in addition to eye tracking, the individualization technique used in our design may have played an essential role in the results obtained. Note that the average FR condition also used an eye-tracking technique; however, IFR could additionally provide personalized vision for each individual. These results show that the current IFR method performed successfully in terms of individualization and was beneficial for maintaining high VE quality with fewer computational resources.

In the SCA group, the effect of the IFR condition differed from the LCA group. In this study, the effect of IFR was less than that of full resolution and similar to the average FR in the main study, and no difference was found across FR conditions in the extension study. Similarly, the effect of the IFR condition was weaker than that of full resolution, with no difference from the average FR in the perception measurements. These results suggest that the SCA participants exhibited relatively insensitive vision. Thus, further consideration of enhancing the VE quality of an SCA group is necessary. However, the IFR methods in this group had effects similar to those of the average FR and required fewer computational resources than the average FR. Overall, the results show that the proposed IFR was useful for saving resources across the two groups.

The demand for graphical realism is rapidly increasing, and finding a balance between rendering resources and the quality of graphical realism is a key necessity in practical applications (Cheung and Legge 2005; Adhanom et al.

2020). Our results emphasize the importance of the proposed IFR method. The proposed IFR method can help developers find a "sweet spot" for each person in terms of deterioration of visual quality and subjective perception. Moreover, the IFR could be more effective in actual applications than in the restricted experimental environment of the main study as shown by the DPQ results from the main and extension studies. The LCA participants did not perceive differences in visual quality in the peripheral areas across the FR conditions in the main study, but they did perceive a difference in the extension study. For example, the main and extension studies varied in terms of the area in which the target objects were arranged. In the main study, we arranged the targets in an area marginally larger than the FoV to evaluate perception based on the visual condition rather than head rotation. In contrast, the targets in the extension study were arranged in an area provided by the VR equipment. Thus, the participants could move their gaze more widely and noticed the latency more easily. Notably, the target area and latency in the extension study showed improved results on the DPQ only under the IFR condition. These results suggest that the proposed IFR method could be expected to perform even better in a real application. In addition, the proposed method could save additional computational resources with an HMD with a wider field of view. By using an HMD that provides 8 K resolution with a 200° diagonal FoV (i.e., Pimax Vision 8 K; Pimax, China), we could reduce the computational resources required by approximately 90%. Interestingly, most computational resources of modern HMDs are allocated to the peripheral area, and the benefits of the proposed IFR method are dramatically greater for wider or high-resolution HMDs.

We found similar patterns across the IFR, average FR, and full-resolution conditions in terms of response time, gaze dispersion, and head rotation between the LCA and SCA groups. The fact that there were no differences in gaze dispersion and head rotation suggests that the behavioral patterns were not significantly different despite the quality deterioration caused by IFR. If peripheral vision was hindered in the IFR condition, the user would have to move either their head or their gaze to find the target. However, the targets could be recognized through the current peripheral vision, and the participants required a similar response time for recognition across all conditions. That is, the behavioral patterns were maintained despite the deterioration of peripheral vision quality in this study, which shows the efficiency of proposed IFR method (i.e., comparable visual experience to FR with fewer computational resources).

We found that the IFR did not have the same effect in the SCA group. The LCA group had similar levels of VEs under the IFR condition compared to the full-resolution condition, which suggests that they had robust vision capability and accurate responses with the proposed method. However,

this was not true in the SCA group, for which we believe there are three potential reasons. One possibility is that the sensitivity of the SCA group in recognizing visual context changes in the static vision condition was lower than that in the dynamic vision conditions with eye movement and head rotation. As we mentioned, studies on ophthalmology have provided two types of visual field tests, including static and dynamic tests, i.e., the Humphrey and Goldmann tests (Goldmann 1946; Trope and Britton 1987; Zahid et al. 2014). Our method is similar to the Goldmann visual field test (Zahid et al. 2014) because the target stimulus moves. The SCA participants who perceived lower quality in the dynamic visual field environment might have experienced some differences in perceiving the quality of the visual fields in a static state. To address this possibility, we propose a lower-bound adjustment of the IFR parameters. Although exact lower-bound values should be measured through further research, our results suggest that effects in terms of inaccurate measurements or late responses could be minimized if we provided average or higher values to individuals in the SCA group. This lower-bound adjustment would also be helpful to compensate for potential measurement failures of some participants. Another possibility is the order in which the parameters were measured could have had some effect. We measured the central area first and then measured the visual quality level of the peripheral vision. Some participants may have a narrow FoV, whereas others may lack the ability to recognize details within their FoV. Human vision is heterogeneous (Cheung and Legge 2005; Murray et al. 2012; Sanda et al. 2018) and variations between individuals must be considered. However, we fixed the quality degradation at a general level and measured the central area first. This may have hindered the precise measurement of the central area in some participants with less ability to perceive quality degradation. Therefore, further experiments should control for the order in which the parameters are measured to confirm any such differences. In addition, the longer response times and higher frequency of errors in the SCA group could be related to the experimental procedure. Although we tried to achieve stable responses from the participants, they could have had difficulties with the responses to the IFR measurement task. This possibility may not have been fully eliminated in this current study. Our results also suggest that participants in the SCA group generally had a slower response time than those in the LCA group.

This study also involves some notable limitations and suggests some promising avenues for future research. First, only two FR parameters (central area and resolution of peripheral area) were used. Because various FR parameters have been proposed in previous studies (Guenter et al. 2012; Vaidyanathan et al. 2014), additional parameter settings that could be individualized should be considered. A larger number of layers or a different order of parameter individualization would be also beneficial for future studies. Second, the participants recruited in this study were young and had no ocular diseases. Although the participants showed sufficient individual differences, our results should be evaluated with more diverse age groups and with participants with visual impairments. Third, different types of quality degradation in the peripheral region or ultra-high-quality rendering in the central region should be investigated along with individualization. Previous studies have suggested some potential approaches to overcome quality degradation (Meng et al. 2020; Park et al. 2022) and achieve realistic rendering (McAuley et al. 2013; Overbeck et al. 2018), which should be investigated along with the proposed individualization method.

8 Conclusion

In this study, we have proposed an IFR method inspired by a medical methodology. Although the IFR technique reduced the rendering resources required to provide a VE, the user VE did not decrease. Humans differ in terms of their peripheral vision depending on individual characteristics, and the proposed method demonstrates the advantages of individualization in FR. The proposed IFR is a flexible technique in terms of rendering efficiency, and provides a useful approach for the future individualization of eye-tracking HMD-based interactions. In the near future, we plan to use wider HMDs, which may require additional computational resources when applying VR. While recognizing the limitations of the empirical contributions of this study, we hope that the results will contribute to the development of new methods and questions and renew enthusiasm for inquiries into individualized VR.

Data availability The datasets generated during the current study are available from the corresponding author on reasonable request.

Declarations

Conflict of interest The authors have no competing interests to declare that are relevant to the content of this article.

References

Adhanom IB, Griffin NN, MacNeilage P, Folmer E (2020) The effect of a foveated field-of-view restrictor on VR sickness. In: 2020 IEEE conference on virtual reality and 3D user interfaces (VR), pp 645–652. https://doi.org/10.1109/vr46266.2020.00087

Adhanom IB, MacNeilage P, Folmer E (2023) Eye tracking in virtual reality: a broad review of applications and challenges. Virtual Real 27:1481–1505. https://doi.org/10.1007/s10055-022-00738-z

Banks MS, Sekuler AB, Anderson SJ (1991) Peripheral spatial vision: limits imposed by optics, photoreceptors, and receptor pooling. J Opt Soc Am A 8(11):1775–1787. https://doi.org/10.1364/josaa.8.001775

Bargary G, Bosten JM, Goodbourn PT, Lawrance-Owen AJ, Hogg RE, Mollon JD (2017) Individual differences in human eye movements: an oculomotor signature? Vision Res 141:157–169. https://doi.org/10.1016/j.visres.2017.03.001

Chen T, Wu YS, Zhu K (2018) Investigating different modalities of directional cues for multi-task visual-searching scenario in virtual reality. In: Proceedings of the 24th ACM symposium on virtual reality software and technology (VRST) '18, pp 1–5. https://doi.org/10.1145/3281505.3281516

Cheung SH, Legge GE (2005) Functional and cortical adaptations to central vision loss. Vis Neurosci 22(2):187–201. https://doi.org/10.1017/s0952523805222071

Derogatis LR, Unger R (2010) Symptom checklist-90-revised. Corsini Encycl Psychol. https://doi.org/10.1002/9780470479216.corpsy0970

Di Luca M (2010) New method to measure end-to-end delay of virtual reality. Presence: Teleoperators Virtual Environ 19(6):569–584. https://doi.org/10.1162/pres_a_00023

Emery KJ, Webster MA (2019) Individual differences and their implications for color perception. Curr Opin Behav Sci 30:28–33. https://doi.org/10.1016/j.cobeha.2019.05.002

Goldmann H (1946) Demonstration unseres neuen projektionskugelperimeters samt theoretischen und klinischen bemerkungen über perimetrie. Ophthalmologica 111(2–3):187–192. https://doi.org/10.1159/000300322

Guenter B, Finch M, Drucker S, Tan D, Snyder J (2012) Foveated 3D graphics. ACM Trans Graph 31(6):1–10. https://doi.org/10.1145/2366145.2366183

Hirzle T, Gugenheimer J, Geiselhart F, Bulling A, Rukzio E (2019) A design space for gaze interaction on head-mounted displays. In: Proceedings of the 2019 CHI conference on human factors in computing systems. CHI '19, pp 1–12. https://doi.org/10.1145/3290605.3300855

Hsu CF, Chen A, Hsu CH, Huang CY, Lei CL, Chen KT (2017) Is foveated rendering perceivable in virtual reality? Exploring the efficiency and consistency of quality assessment methods. In: Proceedings of the 25th ACM international conference on Multimedia. pp 55–63. https://doi.org/10.1145/3123266.3123434

Jacobson SG, Aleman TS, Cideciyan AV, Heon E, Golczak M, Beltran WA, Sumaroka A, Schwartz SB, Roman AJ, Windsor EAM, Wilson JM, Aguirre GD, Stone EM, Palczewski K (2007) Human cone photoreceptor dependence on RPE65 isomerase. Proc Natl Acad Sci 104(38):15123–15128. https://doi.org/10.1073/pnas.0706367104

Jang W, Shin JH, Kim M, Kim K (2016) Human field of regard, field of view, and attention bias. Comput Methods Programs Biomed 135:115–123. https://doi.org/10.1016/j.cmpb.2016.07.026

Kennedy RS, Lane NE, Berbaum KS, Lilienthal MG (1993) Simulator sickness questionnaire: an enhanced method for quantifying simulator sickness. Int J Aviat Psychol 3(3):203–220. https://doi.org/10.1207/s15327108ijap0303_3

Kim M, Kwon T, Kim K (2017) Can human–robot interaction promote the same depth of social information processing as human–human interaction? Int J Soc Robot 10(1):33–42. https://doi.org/10.1007/s12369-017-0428-5

Korkut EH, Surer E (2023) Visualization in virtual reality: a systematic review. Virtual Real. https://doi.org/10.1007/s10055-023-00753-8

Levoy M, Whitaker R (1990). Gaze-directed volume rendering. In: Proceedings of the 1990 symposium on interactive 3D graphics—SI3D '90. https://doi.org/10.1145/91385.91449

Lin JJW, Duh HBL, Parker DE, Abi-Rached H, Furness TA. (2002) Effects of field of view on presence, enjoyment, memory, and simulator sickness in a virtual environment. In: Proceedings IEEE virtual reality 2002. pp 164–171. https://doi.org/10.1109/vr.2002.996519

Masnadi S, Pfeil K, Sera-Josef JVT, LaViola J (2022) Effects of field of view on egocentric distance perception in virtual reality. In: CHI conference on human factors in computing systems. CHI '22. pp 1–10. https://doi.org/10.1145/3491102.3517548

McAuley S, Hoffman N, Zap Andersson H, Hill S, Martinez A, Villemin R, Pettineo M, Lazarov D, Neubelt D, Karis B, Hery C (2013) Physically based shading in theory and practice. In: ACM SIGGRAPH 2013 courses. pp 1–8. https://doi.org/10.1145/2504435.2504457

Meng X, Du R, Varshney A (2020) Eye-dominance-guided foveated rendering. IEEE Trans vis Comput Graph 26(5):1972–1980. https://doi.org/10.1109/tvcg.2020.2973442

Murray IJ, Parry NRA, McKeefry DJ, Panorgias A (2012) Sex-related differences in peripheral human color vision: a color matching study. J vis 12(1):1–10. https://doi.org/10.1167/12.1.18

Navarro R, Williams DR, Artal P (1993) Modulation transfer of the human eye as a function of retinal eccentricity. J Opt Soc Am A 10(2):201–212. https://doi.org/10.1364/josaa.10.000201

Ogboso YU, Bedell HE (1987) Magnitude of lateral chromatic aberration across the retina of the human eye. J Opt Soc Am A 4(8):1666–1672. https://doi.org/10.1364/josaa.4.001666

Overbeck RS, Erickson D, Evangelakos D, Pharr M, Debevec P (2018) A system for acquiring, processing, and rendering panoramic light field stills for virtual reality. ACM Trans Graph 37(6):1–15. https://doi.org/10.1145/3272127.3275031

Pai YS, Dingler T, Kunze K (2019) Assessing hands-free interactions for VR using eye gaze and electromyography. Virtual Real 23:119–131. https://doi.org/10.1007/s10055-018-0371-2

Park SH, Han B, Kim GJ (2022). Mixing in reverse optical flow to mitigate vection and simulation sickness in virtual reality. In: CHI conference on human factors in computing systems. CHI '22, pp 1–11. https://doi.org/10.1145/3491102.3501847

Patney A, Salvi M, Kim J, Kaplanyan A, Wyman C, Benty N, Luebke D, Lefohn A (2016) Towards foveated rendering for gaze-tracked virtual reality. ACM Trans Graph 35(6):1–12. https://doi.org/10.1145/2980179.2980246

Sanda N, Cerliani L, Authié CN, Sabbah N, Sahel JA, Habas C, Safran AB, Thiebaut de Schotten M (2018) Visual brain plasticity induced by central and peripheral visual field loss. Brain Struct Funct 223(7):3473–3485. https://doi.org/10.1007/s00429-018-1700-7

Sekuler AB, Bennett PJ, Mamelak M (2000) Effects of aging on the useful field of view. Exp Aging Res 26(2):103–120. https://doi.org/10.1080/036107300243588

Sheridan TB (1992) Musings on telepresence and virtual presence. Presence: Teleoperators Virtual Environ 1(1):120–126. https://doi.org/10.1162/pres.1992.1.1.120

Stengel M, Grogorick S, Eisemann M, Eisemann E, Magnor MA (2015) An affordable solution for binocular eye tracking and calibration in head-mounted displays. In: Proceedings of the 23rd ACM international conference on multimedia. MM '15, pp 15–24. https://doi.org/10.1145/2733373.2806265

Strasburger H, Rentschler I, Juttner M (2011) Peripheral vision and pattern recognition: a review. J vis 11(5):1–82. https://doi.org/10.1167/11.5.13

Swafford NT, Iglesias-Guitian JA, Koniaris C, Moon B, Cosker D, Mitchell K (2016) User, metric, and computational evaluation of foveated rendering methods. In: Proceedings of the ACM symposium on applied perception. SAP '16, pp 7–14. https://doi.org/10.1145/2931002.2931011

Tian N, Lopes P, Boulic R (2022) A review of cybersickness in head-mounted displays: raising attention to individual susceptibility. Virtual Real 26(4):1409–1441. https://doi.org/10.1007/s10055-022-00638-2

Trope GE, Britton R (1987) A comparison of Goldmann and Humphrey automated perimetry in patients with glaucoma. Br J Ophthalmol 71(7):489–493. https://doi.org/10.1136/bjo.71.7.489

Usoh M, Catena E, Arman S, Slater M (2000) Using presence questionnaires in reality. Presence: Teleoperators Virtual Environ 9(5):497–503. https://doi.org/10.1162/105474600566989

Vaidyanathan K, Salvi M, Toth R, Foley T, Akenine-Möller T, Nilsson J, Munkberg J, Hasselgren J, Sugihara M, Clarberg P, Janczak T, Lefohn A (2014) Coarse pixel shading. In: Proceedings of high performance graphics. pp 9–18. https://doi.org/10.2312/HPG.20141089

Van Dam LCJ, Stephens JR (2018) Effects of prolonged exposure to feedback delay on the qualitative subjective experience of virtual reality. PLoS ONE 13(10):e0205145. https://doi.org/10.1371/journal.pone.0205145

Wald G (1945) Human vision and the spectrum. Science 101(2635):653–658. https://doi.org/10.1126/science.101.2635.653

Welch RB, Blackmon TT, Liu A, Mellers BA, Stark LW (1996) The effects of pictorial realism, delay of visual feedback, and observer interactivity on the subjective sense of presence. Presence: Teleoperators Virtual Environ 5(3):263–273. https://doi.org/10.1162/pres.1996.5.3.263

Witmer BG, Singer MJ (1998) Measuring presence in virtual environments: a presence questionnaire. Presence: Teleoperators Virtual Environ 7(3):225–240. https://doi.org/10.1162/105474698565686

Xiao K, Liktor G, Vaidyanathan K (2018) Coarse pixel shading with temporal supersampling. In: Proceedings of the ACM SIGGRAPH symposium on interactive 3D graphics and games (I3D) '18. https://doi.org/10.1145/3190834.3190850

Zahid S, Peeler C, Khan N, Davis J, Mahmood M, Heckenlively JR, Jayasundera T (2014) Digital quantification of Goldmann visual fields (GVFs) as a means for genotype–phenotype comparisons and detection of progression in retinal degenerations. Retin Degener Dis 801:131–137. https://doi.org/10.1007/978-1-4614-3209-8_17